Electronic Spectra of Jet-Cooled 3- and 4-Chlorotropolones : Influence of Asymmetric Substitution on the Intramolecular Hydrogen Bonding

Tsuji, Takeshi
Department of Molecular Science and Technology Grauate School of Engineering Sciences

Sekiya, Hiroshi
Institute of Advanced Material Study Kyushu University

Ito, Sayaka
Department of Molecular Science and Technology Grauate School of Engineering Sciences

Ujita, Hiroki
Institute of Advanced Material Study Kyushu University

他

https://doi.org/10.15017/6619

出版情報：九州大学機能物質科学研究所報告. 7 (1), pp.1-14, 1993-09-30. Institute of Advanced Material Study Kyushu University
バージョン：
権利関係：

Rep.Inst.Adv.Mat.
Study, Vol. 7 No. 1
pp. 1 ~ 14(1993)

Electronic Spectra of Jet-Cooled 3- and 4-Chlorotropolones. Influence of Asymmetric Substitution on the Intramolecular Hydrogen Bonding

Takeshi TSUJI,* Hiroshi SEKIYA, Sayaka ITO,*
Hiroki UJITA, Mariko HABU,* Akira MORI,
Hitoshi TAKESHITA, and Yukio NISHIMURA

The fluorescence excitation and fluorescence spectra of jet-cooled 3-chlorotropolone (3CTR-*h*) and 4-chlorotropolone (4CTR-*h*) were measured in the S_1-S_0 region. Several transitions of 3CTR-*h* have been identified in the region of 26403-26694 cm^{-1}, whereas only the origin band has been detected at 26338 cm^{-1} in 4CTR-*h*. No tunneling splitting was observed in the both spectra, suggesting that the hydroxylic proton is localized almost completely in one well of an asymmetric double-minimum potential function along the proton transfer coordinate. The vibronic structure in the fluorescence excitation spectrum of 4CTR-*h* is extremely different from that of 3CTR-*h*, which is ascribed to the change of the geometry in S_1 of 4CTR-*h*.

Introduction

Tropolone (TRN-*h*) has an intramolecular hydrogen bond, and its hydroxylic proton is delocalized between two oxygen atoms in both the S_0 and S_1 states.[1-3] The asymmetric substitution on the seven-membered ring of TRN-*h* will cause the localization of the proton. Previously, we have reported the S_1-S_0 electronic spectra of asymmetric derivatives, 3-bromotropolone (3BTR-*h*),[4] 3-isopropyltropolone (3IPT-*h*),[5] and 4-

Received May 20, 1993
* Department of Molecular Science and Technology, Grauate School of Engineering Sciences

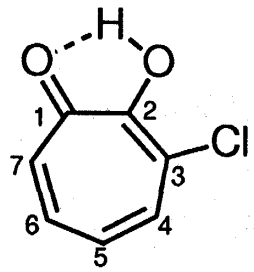

3CTR

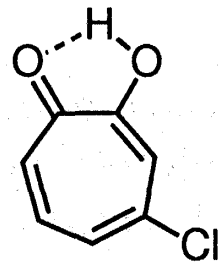

4CTR

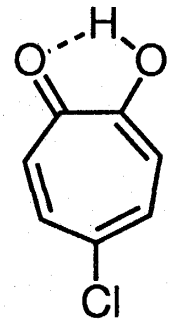

5CTR

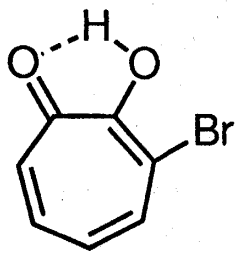

3BTR

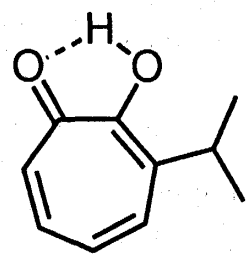

3IPT

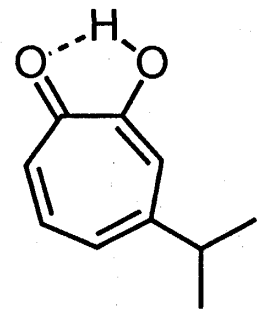

4IPT

isopropyltropolone (4IPT-*h*)[5] in supersonic free-jets. We concluded that the hydroxylic proton is almost completely localized in 3BTR-*h*[4] and 4IPT-*h*[5] since no tunneling splitting was observed. On the other hand, the 0_1^+ transition[6] shown in Fig. 1a was observed in the fluorescence excitation spectrum of 3IPT-*h*,[5] suggesting that the degree of the localization of proton in 3IPT-*h* must be small as compared with those of 3BTR-h and 4IPT-*h*. Thus the effect of the asymmetric substitution on the motion of the hydroxylic proton strongly depends on the substituents and their positions. Further studies are needed for comprehensive understanding.

In this paper, we have measured the 3CTR and 4CTR spectra to investigate the asymmetric substitution of a Cl atom on the intramolecular hydrogen bonding. No sign of the proton tunneling has been observed in the fluorescence excitation spectra of 3CTR-*h* and 4CTR-*h*. This suggests that the hydroxylic protons of 3CTR-*h* and 4CTR-*h* are considered to be localized in one well. The vibronic structure in the fluorescence excitation spectrum of 4CTR-*h* has been found to be very different from that of 3CTR-*h*. Only the origin band has been detected, probably due to significant change in the geometry in S_1 of 4CTR-*h*.

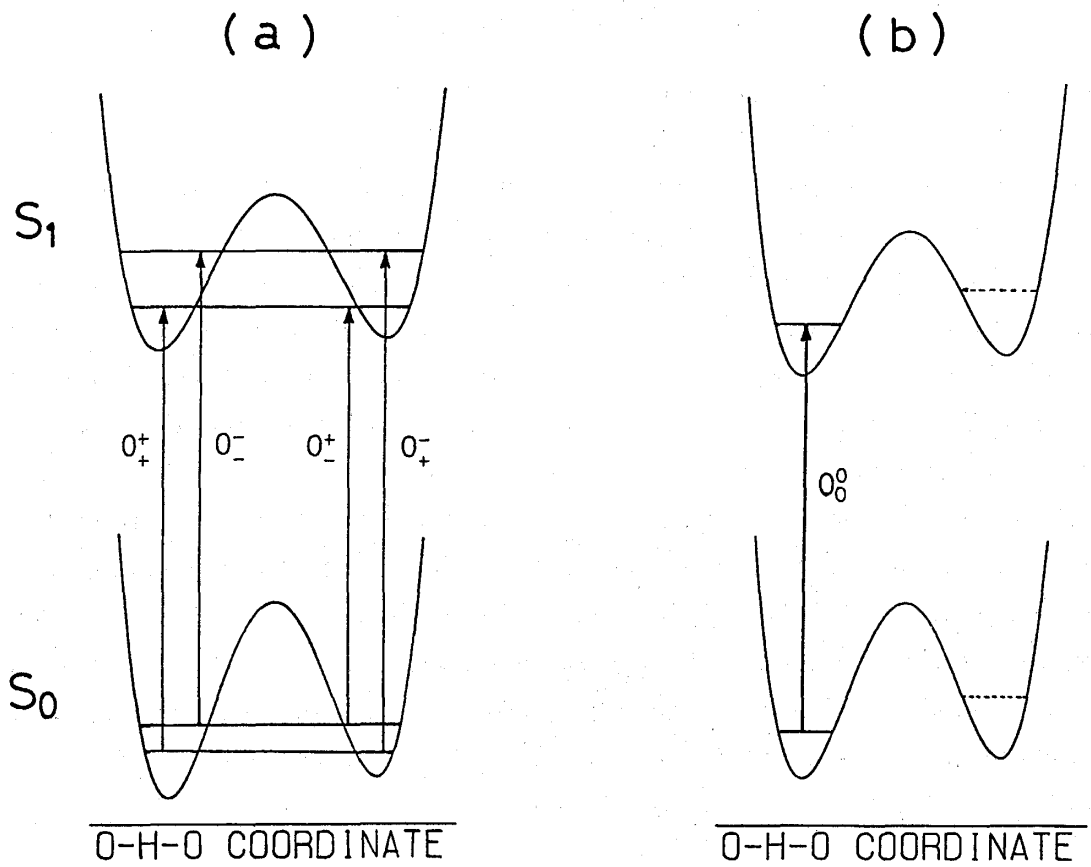

Fig. 1 : Schematic drawing of asymmetric double-minimum potential functions along the proton transfer coordinate. The 0^+ and 0^- wavefunctions are partially localized in (a), whereas completely localized in (b).

Experimental

The experimental apparatus used is essentially the same as that reported previously.[3-5] 3CTR-*h* and 4CTR-*h* were synthesized by using known methods.[7, 8] The samples were purified by recrystallization and sublimation, but we could not exclude very small amount of 5CTR-*h* produced in the process of the 3CTR-*h* preparation. The sample in the nozzle housing was heated to 120-130℃ to increase the vapor pressure. 3CTR-*d* and 4CTR-*d* were prepared by introducing a trace of water into the nozzle housing. The excitation source was a nitrogen-laser-pumped dye laser system (Molectron UV22 and DL14). A solution of a mixture of BBQ and PBD dyes with molar concentration ratio BBQ / PBD = 3 / 2 was used. Dispersed fluorescence spectra were measured with a f = 0.75 m monochrometor (Spex 1702). The fluorescence was detected with a photomultiplier tube (Hamamatsu R955), stored on a storage scope (Philips PM3323) and collected on an NEC PC9801 microcomputer. The spectra were normalized by the laser intensity.

Results and Discussion

Fluorescence excitation and dispersed fluorescence spectra of 3CTR. In addition to the vibronic bands of 5CTR-*h* in the region of 26009-26409 cm^{-1}, several vibronic bands are detected in Fig. 2. We can easily find a prominent progression with intervals about 50 cm^{-1}. This progression corresponds to the lowest-frequency out-of-plane bending mode ν'_{26} of TRN-*h*.[1-3] Similar progressions of ν'_{26} have been also observed in the fluorescence excitation spectra of 5BTR-*h*, 5CTR-*h*, and their OD derivatives.[9] The bands at $\Delta\tilde{\nu} = 0$ and 51 cm^{-1} had been assigned to the intramolecular hydrogen-bonded complex between 3CTR-h and water,[10] since the intensities of these bands increased with the introduction of a trace of water. However, the band at $\Delta\tilde{\nu} = 0$ cm^{-1} ($\tilde{\nu} = 26403 cm^{-1}$) should be assigned as the origin band of 3CTR-*h* on the basis of the measurement of the dispersed fluorescence spectrum, which will be shown later. By analogy with the fluorescence spectrum of TRN-*h*, 5BTR-*h*, and 5CTR-*h*, the bands at $\Delta\tilde{\nu} = 51$, 105, and 158 cm^{-1} could be assigned as the 26_0^2, 26_0^4, and 26_0^6 transitions, respectively. Two strong bands have been detected at $\Delta\tilde{\nu} = 286$ and 291 cm^{-1}. Although we could not assign definitely, these bands might be due to in-plane ring-deformation mode corresponding to ν'_{13} and / or ν'_{14} modes of TRN-*h*[1-3] from the frequencies.

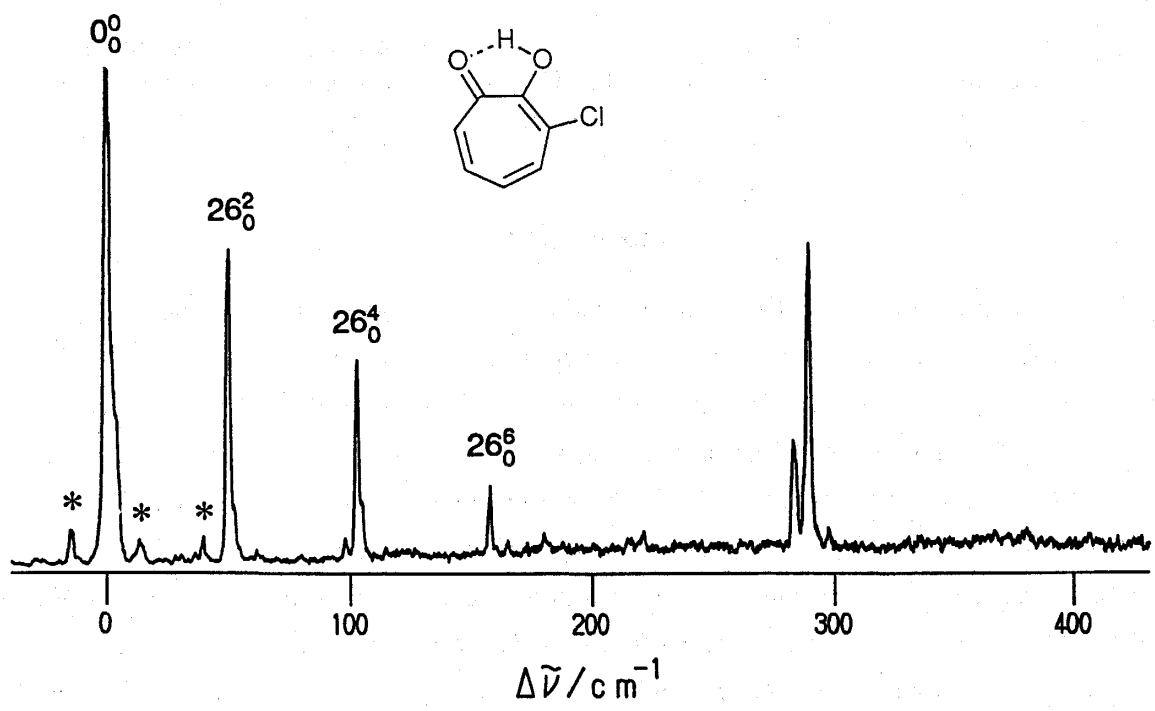

Fig. 2 : Fluorescence excitation spectrum of 3CTR-*h* in a supersonic free jet. The stagnation pressure of He was 1 atm. The bands indicated by asterisks are due to 5CTR-h.

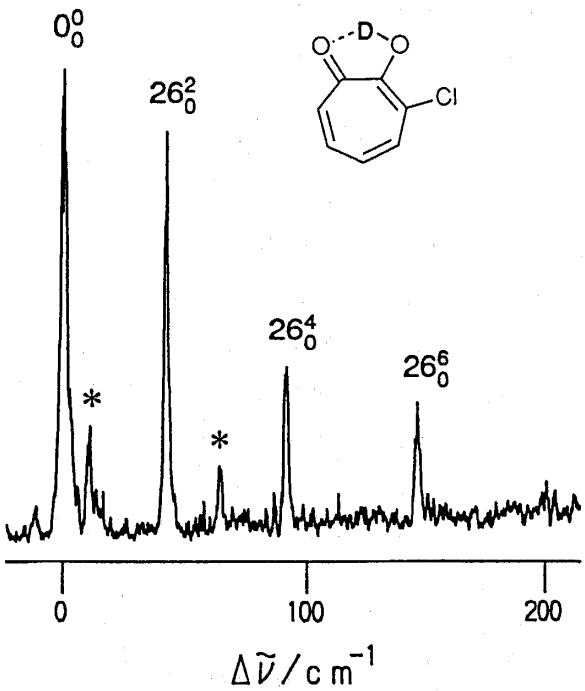

Fig. 3 : Fluorescence excitation spectrum of 3CTR-*d* in a supersonic free jet. The stagnation pressure of He was 1 atm. The bands indicated by asterisks are due to 3CTR-*h*.

Figur 3 shows the fluorescence excitation spectrum of 3CTR-*d*. The electronic origin band is identified at $\tilde{\nu} = 26444\,cm^{-1}$, which is $41\,cm^{-1}$ blue shifted from that of 3CTR-*h*. The intervals of the ν'_{26} progression have decreased by $10\,cm^{-1}$ upon deuteration. The bands at $\Delta\tilde{\nu} = 41, 92$, and $146\,cm^{-1}$ can be assigned as the 26_0^2, 26_0^4, and 26_0^6 transitions, respectively. The wave numbers and assignments are summarized in Table 1.

In the fluorescence excitation spectra of TRN-h,[1-3] 3IPT-*h*,[5] 5BTR-*h*, and 5CTR-*h*,[9] the tunneling splittings have been observed. In these molecules, the magnitude of the tunneling splitting decreased drastically upon deuteration because of the increase in the reduced mass. Such an isotope effect is not observed in Figs. 2 and 3. The nonobservation of the tunneling splitting suggests that the hydroxylic proton in 3CTR-*h* is almost completely localized in one well of the asymmetric

Table 1. Wave numbers for vibronic bands detected in the laser fluorescence excitation spectra of 3CTR-*h* and 3CTR-*d* (cm^{-1}).

Molecule	$\tilde{\nu}$	$\Delta\tilde{\nu}$	Assignments
3CTR-*h*	26403	0	0_0^0
	26454	51	26_0^2
	26508	105	26_0^4
	26561	158	26_0^6
	26689	286	
	26694	291	
3CTR-*d*	26444	0	0_0^0
	26485	41	26_0^2
	26536	92	26_0^4
	26590	146	26_0^6

double-minimum potential in both the S_0 and S_1 states, as is the case for 3BTR-*h*.[4] An asymmetric double-minimum potential function along the proton transfer coordinate for 3CTR-*h* is schematically shown in Fig. 1b. The zero-point level in S_0 of the right side potential in Fig. 1b is considered to be thermally inaccessible in the cold jet.

In Fig. 4 is shown a typical dispersed fluorescence spectrum of 3CTR-*h* obtained by exciting the electronic origin band. A lot of vibrational modes are detected in Fig. 3, and the vibronic pattern in the dispersed fluorescence spectrum of 3CTR-h is very similar to those of 5CTR-*h*[9] and TRN-*h*[1-3] obtained by exciting the 0^{+}_{+} and 0^{-}_{-} transitions. This result is consistent with the assignment of the origin band in Fig. 1. Vibrational assignments were made by analogy with the dispersed fluorescence spectra of TRN-*h*[1-3] and 5CTR-*h*,[9] and are listed in Table 2 together with the Raman data.

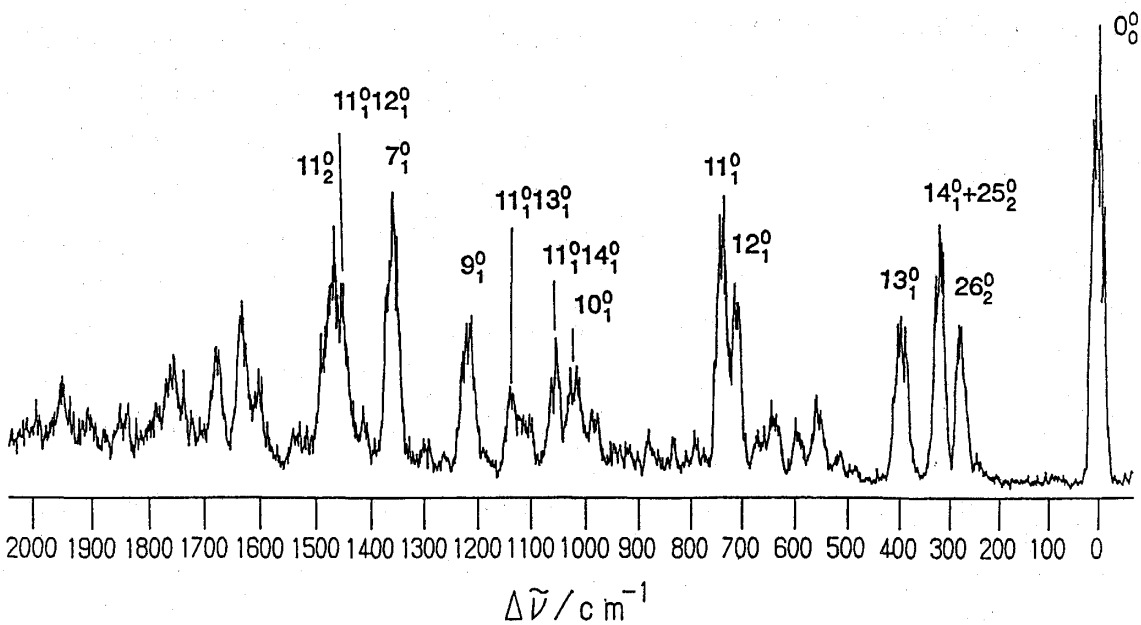

Fig. 4 : Dispersed fluorescence spectrum of 3CTR-*h* obtained by exciting the electronic origin band ($\tilde{\nu} = 26403 cm^{-1}$).

Table 2. Emission bands for 3CTR-*h* obtained by the excitation of the 0_0^0 transition (cm^{-1}).

$\Delta\tilde{\nu}$	Raman[a]	Assignments
0		
($\tilde{\nu}$=26403)		
276		26_2^0
321	310	$14_1^0+25_2^0$
395	378	13_1^0
557		
596		
642		
708	715	12_1^0
737	750	11_1^0
987		
1018	1007	10_1^0
1050		$11_1^0 14_1^0$
1138		$11_1^0 13_1^0$
1213	1232	9_1^0
1359	1360	7_1^0
1453	1450	$11_1^0 12_1^0$
1468		11_2^0
1601	1602	
1631		
1677		
1756		
1951		

[a] Measured in the sold state.

Fluorescence excitation and dispersed fluorescence spectra of 4CTR. In Fig. 5 is shown the fluorescence excitation spectrum of 4CTR-*h* in the region $\Delta\tilde{\nu}$ = 26330-26480 cm^{-1}. In contrast with the fluorescence excitation spectra of 5CTR-*h* and 3CTR-*h*, no ν'_{26} progression is observed. We assigned the band at $\tilde{\nu}$ = 26338 cm^{-1} to the electronic band origin by measuring the dispersed fluorescence spectrum shown in Fig. 6. Various vibrational mode has been identified in Fig. 6. The vibrational modes observed in Fig. 6 have been detected in the dispersed fluorescence spectra of 5TRN-*h*, 5CTR-*h*, and 3CTR-*h* obtained by exciting the origin bands. This result is consistent with the assignment of the 0_0^0 band in Fig. 6. The frequencies of the observed bands and assignments are summa-

rized in Table 3.

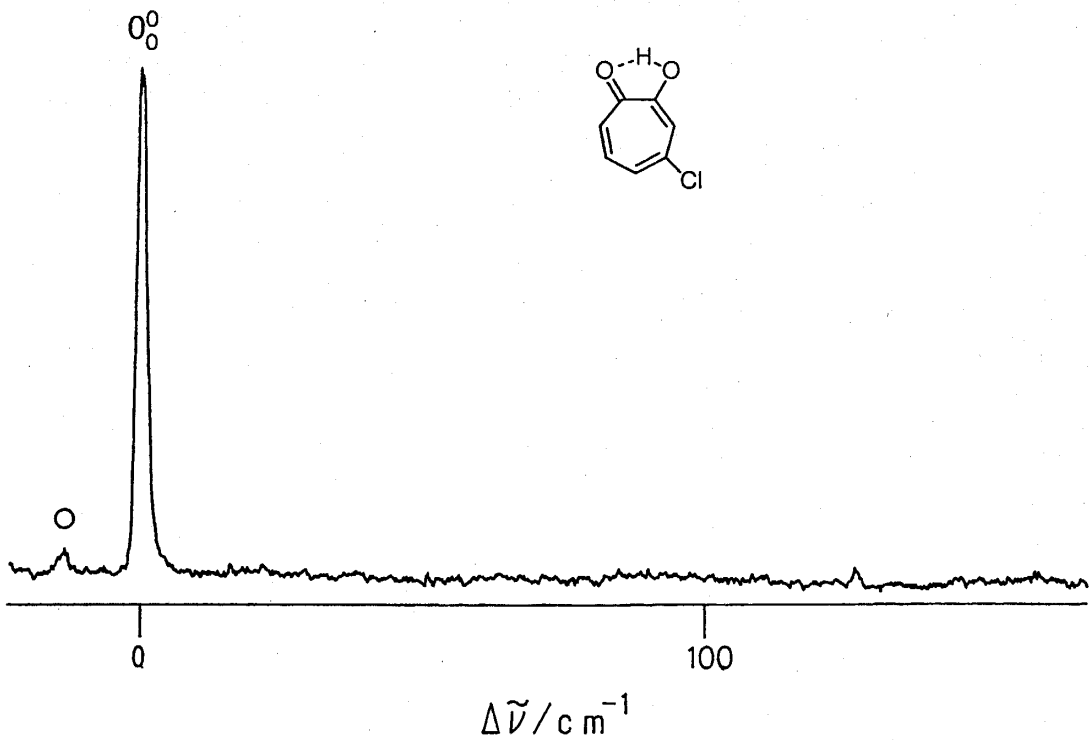

Fig. 5 : Fluorescence excitation spectrum of 4CTR-*h*. The stagnation pressure of helium was 1 atm. The band indicated by the open circle is due to 5CTR-*h* is involved in 4CTR-*h* as an impurity.

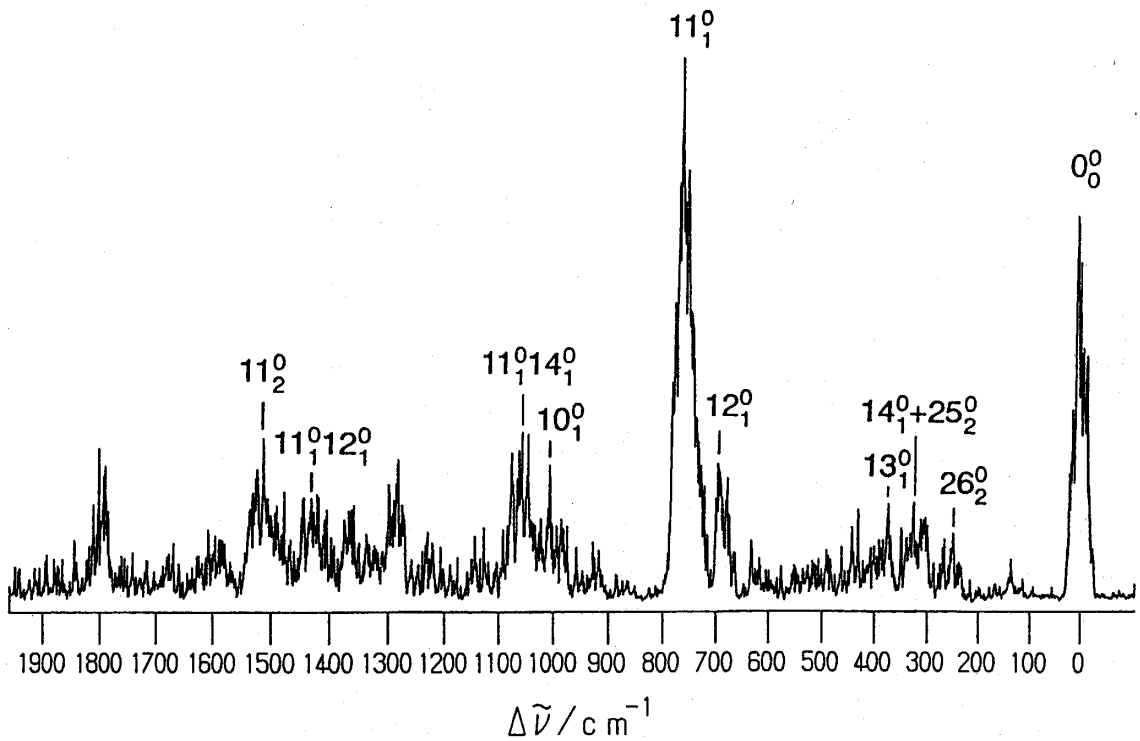

Fig. 6 : Dispersed fluorescence spectrum of 4CTR-*h* obtained by exciting the electronic origin band in Fig. 5.

Table 3. Emission bands for 4CTR-*h* obtained by the excitation of the 0_0^0 transition (cm^{-1}).

$\Delta\tilde{\nu}$	Raman[a]	Assignments
0		
($\tilde{\nu}$=26338)		
255	255	26_2^0
315	315	$14_1^0+25_2^0$
375	365	13_1^0
687		12_1^0
760	760	11_1^0
1005	1005	10_1^0
1059		$11_1^0 14_1^0$
1285	1280	
1365		
1429	1440	$11_1^0 12_1^0$
1512		11_2^0
1597	1600	
1795		

[a] Measured in the solid state.

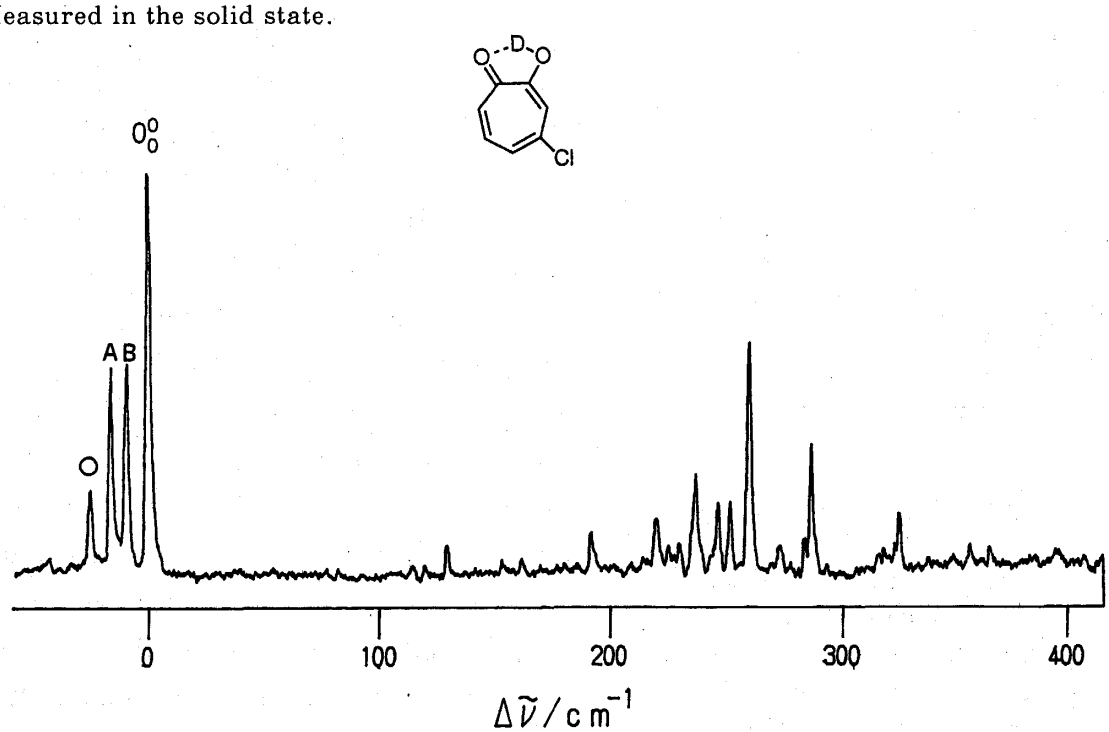

Fig. 7 : Fluorescence excitation spectrum of 4CTR-*d*. The stagnation pressure of helium was 1 atm. The band marked with the open circle is due to 5CTR-*d*. The bands A and B are due to unidentified impurity (see the text).

Table 4. Wavenumbers for vibronic bands detected in the laser fluorescence excitation spectra of 4CTR-*h* and 4CTR-*d* (cm^{-1}).

Molecule	$\tilde{\nu}$	$\Delta\tilde{\nu}$	Assignments
4CTR-*h*	26338	0	0_0^0
4CTR-*d*	26346	−17	impurity
	26353	−10	impurity
	26363	0	0_0^0
	26601	238	
	26610	247	
	26616	253	
	26624	261	
	26650	287	

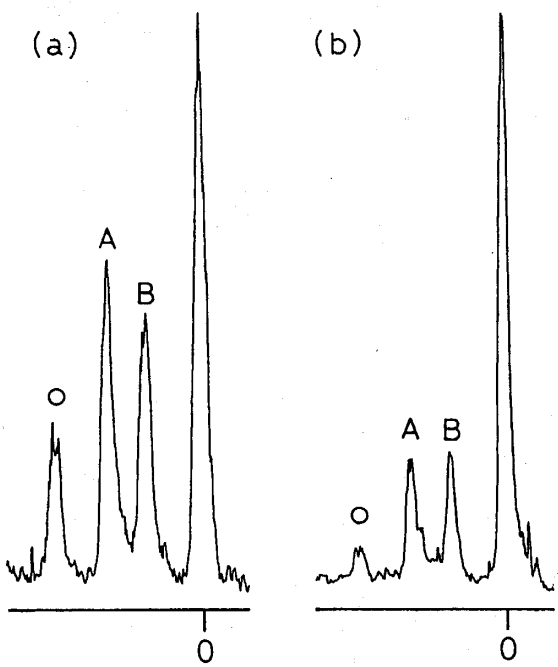

Fig. 8 : Time dependence of the fluorescence excitation spectrum of 4CTR-*d* around the region of the electronic origin band. The spectrum (a) was measured thirty minutes after the input of D_2O, while the spectrum (b) was measured after three hours.

The fluorescence excitation spectrum of 4CTR-*d* is shown in Fig. 7. In addition to the strongest band assigned as 0_0^0 at $\Delta\tilde{\nu} = 0$ ($\tilde{\nu}$ = 26363 cm^{-1}), two bands marked A and B have been detected in the lower wave number region. The wave numbers for these bands are summarized in Table 4. Since similar bands have not been detected in 5CTR-*d*[9] and 3CTR-*d*, we considered these bands are due to impurity. In order to confirm the assumption, we measured the time dependence of the relative intensities of the A and B bands to the intensity of the origin band. Figur 8a shows the fluorescence excitation spectrum for which we started measurements 30 minutes after the introduction of D_2O, while Fig. 8b is obtained after 3 hours. The relative intensities of the bands A and B has decreased remarkably as compared with the intensity of the origin band. This suggests that the bands A and B are not the vibronic bands of 4CTR-*d*. The candidates for the impurity which provided the bands A and B are deuterated 4CTR molecules for which the deuterium

atom (s) is substituted in the skeletal seven-membered ring[11] in the reaction of 4CTR-*h* with D_2O, because these bands appear only when D_2O was input in the heated nozzle housing. Further study is needed to assign the bands A and B definitely.

It is clear from Figs. 5 and 7 that no tunneling doublet component is observed. This suggests that the hydroxylic proton is localized in both S_0 and S_1. We concluded that the double-minimum potential well for 4CTR is asymmetric as schematically shown in Fig. 1b. Among the three chlorinated molecules studied by us, proton tunneling has been observed only in the symmetrically substituted 5CTR molecule.[9] We observed the 0_0^+ transition in the fluorescence excitation spectra of asymmetrically substituted molecules 3IPT-*h* and 3IPT-*d*.[5] These observations indicates that the degree of asymmetry in the double minimum potential well is larger for 4CTR and 3CTR than that for 3IPT due to larger electronic effect of the chlorine atom than the isopropyl group on the intramolecular hydrogen bond. Since the number of electrons in the Cl atom is much larger than the C atom of the isopropyl group which is bonded with the C atom at 3- or 4- position, the Cl atom can supply more charge on the seven-membered ring, which will affect the strength of the intramolecular hydrogen bonding. Only a slight lowering of the symmetry from C_{2v} prevents efficient proton tunneling in the case of 4CTR.

The vibronic structures of 4CTR-*h* and 4CTR-*d* are completely different from those of 5CTR-*h* and 3CTR-*h* and their deuterated molecules,[9] respectively. The remarkable change of the vibronic structure is probably due to significant change of the molecular geometry in the S_1 state, since the vibrational frequencies in the S_0 state of 4CTR-*h* is similar to those of 4CTR-*h* and 3CTR-*h*. The change of the geometry in S_1 will make the Franck-Condon overlapping between S_0 and S_1 poor.

The ν'_{26} progression. The ν'_{14} progression has been observed in the fluorescence excitation spectra of 3CTR-*h*, 5CTR-*h*, and 5BTR-*h*.[9] We have already reported the fluorescence excitation spectra of 3BTR-*h* and 3BTR-*d*.[4] Several low-frequency bands were detected in the excitation spectra. In the previous work we could not assign the vibronic bands definitely becaus of the lack of enough information about the chang of the frequency for the ν'_{26} mode when the bromine atom is substituted. In this work, with the aid of the assignments in the spectra of 5CTR-*h*, 3CTR-*h*, and 5BTR-*h*, we can assign several vibronic bands involving the ν'_{26} mode in the 3BTR-*h* and 3BTR-*d* spectra. The assignments are summarized in Table 5. Similarly, the band at $\Delta\tilde{\nu} = 270\,cm^{-1}$ in the dispersed fluorescence spectrum of 3BTR-*h* can be assigned as 26_2^0. The ν'_{26} (b_1) mode in TRN-*h* has been considered to be an out-of-plane bending mode involving the motion of the O..H..O chelate group.[1-3] Very recently, the displacements for the Q''_{26} normal coordinates were calculated at the 6-31G level by Redington and Bock.[12] According to their calculations the displacements of the hydrogen atoms at 4-, 5-, and 6-positions are

Table 5. Vibrational assignments for bands in the fluorescence excitation spectrum of 3BTR-*h* and 3BTR-*d*.

Molecule	$\tilde{\nu}$	$\Delta\tilde{\nu}$	Assignments
3BTR-*h*	26289	−21	hot band
	26300	−10	hot band
	26310	0	0_0^0
	26345	35	26_0^2
	26389	79	26_0^4
	26407	97	
	26438	128	26_0^6
3BTR-*d*	26319	−23	hot band
	26342	0	0_0^0
	26368	26	26_0^2
	26411	69	26_0^4
	26423	81	
	26458	116	26_0^6

Table 6. Vibrational constants for the ν'_{26} mode (cm^{-1}) in S_1. *s* stands for standard variance.

Molecule	$\omega_{26}^0 + x_{26}^0$	ω_{26}^0	x_{26}^0	*s*
TRN-*h*	35.4	36.1	−0.4	2.0
5CTR-*h*	33.7	33.6	0.1	−
5BTR-*h*	18.6	18.4	0.2	1.2
3CTR-*h*	25.7	25.5	0.1	0.5
3BTR-*h*	16.9	16.0	0.9	0.5

very large in Q''_{26}. This reflects that the frequency of ν'_{26} will change significantly when the hydrogen atom at 3-, 4-, and 5-position is substituted by a heavy atom such as the chlorine and bromine atoms.

The vibrational constants for 3CTR-*h* are listed in Table 6 together with those for TRN-*h*, 5CTR-*h*, 5BTR-*h*, and 3BTR-*h*. These values are obtained by using the equation

$$\tilde{\nu} = \omega_{26}^0 v + x_{26}^0 v^2.$$

We defined the vibrational frequency in the S_1 state with quantum number *v* as

$$\tilde{\nu} = \Delta\tilde{\nu}\,(26_0^{v\,\pm}) + (\Delta'_v - \Delta'_0)/2,$$

where $\Delta\tilde{\nu}\,(26_0^{v\,\pm})$ is the interval between the $26_0^{v\,\pm}$ and $0_0^{\pm}$ transitions, Δ'_v is the tunneling doublet separation in the 26_0^v transition.

We noted that the ω' values of 3CTR-*h* (25.5 cm^{-1}), 3BTR-*h* (16.9 cm^{-1}), 5BTR-*h* (18.4 cm^{-1}) decreased drastically from the values of TRN-*h* (36.1 cm^{-1}) due to the substitution of a halogen atom. On the other hand, the ω' value of 5CTR-*h* (33.6 cm^{-1}) decreased slightly from the value of TRN-h as compared with the cases of 3CTR-*h*, 3BTR-*h*, and 5BTR-*h*. The small decrease in the ω' value for 5CTR-h will be ascribed to the increase of the reduced mass. However, the change in the ω' value of 3CTR-*h*, 3BTR-*h*, 5BTR-*h*, are too large to be ascribed to the change in the reduced mass. Such a great change in the vibrational frequency could be ascribed to the change in the Q'_{26} in the S_1 states of these molecules from that of TRN-*h*. The ω' values fof 3CTR-h and 3BTR-h are smaller than those for 5CTR-h and 5BTR-h, respectively, suggesting that the contribution of the chlorine or bromine atom at 3- position is larger than the atom at 5-position to the reduced mass of the ν'_{26} mode.

The vibrational fundamentals of the ν''_{26} mode in the S_0 states of TRN-*h*, 5BTR-*h*, 5CTR-*h*, 3BTR-*h*, and 3CTR-*h* have been measured to be 109, 120, 122, 135, and 138 cm^{-1},[3, 9] respectively. In contrast with the remarkable changes in the ω' values in the S_1 states of bromotropolones and chlorotropolones, the differences in the frequency from the ω'' value of TRN-*h* are much smaller in the S_0 states. This suggests that the changes in the Q'_{26} coordinate of 3CTR-*h*, 3BTR-*h*, and 5BTR-*h* occur upon electronic excitation. The vibrational fundamentals in the S_0 states decrease significantly in the S_1 state for all the molecules, suggesting that the bending motion occurs easily in the S_1 states.

Conclusion

The electronic spectra of 3CTR and 4CTR have been investigated. No tunneling splitting has been observed in the fluorescence excitation spectra of 3CTR-*h*, 4CTR-*h*, and their OD derivatives. The hydroxylic proton is almost completely localized in one well in the asymmetric double-minimum potential function for all molecules studied in this work. The vibronic structure of 4CTR is very different from those of 3CTR and 5CTR. Significant change of the molecular geometry in S_1 of 4CTR has been suggested.

The authors wish to thank Dr. Masaaki Fujii (Department of Chemistry, Tohoku University) for valuable suggestions. We also thank to Dr. Yasuhiko Gondo (Department oF Chemistry, Kyushu University) for allowing us to use a Raman spectrometer. This work was supported in part by Asahi Glass Foundation and the Casio Science Foundation.

References

1) A. C. P. Alves, J. M. Hollas, H. Musa, and T. Ridley, *J. Mol. Spectrosc.*, **109**, 99 (1985).

2) R. L. Redington, Y. Chen, G. J. Scherer, and W. Field, *J. Chem. Phys.*, **88**, 627 (1988).

3) (a) H. Sekiya, Y. Nagashima, and Y. Nishimura, *J. Chem. Phys.*, **92**, 5761 (1990) ; (b) H. Sekiya, Y. Nagashima, and Y. Nishimura, *Bull. Chem. Soc.* Jpn., **62**, 3229 (1989) ; (c) H. Sekiya, Y. Nagashima, T. Tsuji, Y. Nishimura, A. Mori, and H. Takeshita, *J. Phys. Chem.*, **95**, 10311 (1991).

4) H. Sekiya, K. Sasaki, Y. Nishimura, A. Mori, and H. Takeshita, *Chem. Phys. Lett.*, **174**, 133 (1990).

5) (a) H. Sekiya, H. Takesue, Y. Nishimura, Z. H. Li, A. Mori, and H. Takeshita, *Chem. Lett.*, **1988**, 1601 ; (b) H. Sekiya, H. Takesue, Y. Nishimura, Z. H. Li, A. Mori, and H. Takeshita, *J. Chem. Phys.*, **92**, 2790 (1990).

6) (a) R. Rossetti, R. Rayford, R. C. Haddon, and L. E. Brus, *J. Am. Chem. Soc.*, **103**, 4303 (1981) ; (b) G. D. Gillispie, M. H. Van Benthem, and M. Vangsness, *J. Phys. Chem.*, **90**, 2596 (1986) ; (c) P. F. Barbara, P. K. Walsh, and L. E. Brus, *J. Phys. Chem.*, **93**, 29 (1989).

7) T. Nozoe, S. Seto, M. Ito, M. Sato, and T. Katono, *Sci. Rep. Tohoku Univ.*, I **37**, 191 (1953).

8) T. Sato, *J. Chem. Soc. Jpn.*, **80**, 1171 (1959).

9) T. Tsuji, H. Sekiya, Y. Nishimura, Y. Mori, R. Mori, A. Mori, and H. Takeshita, *J. Chem. Phys.*, **97**, 6032 (1992).

10) T. Tsuji, H. Sekiya, Y. Nishimura, A. Mori, and H. Takeshita, *J. Chem. Phys.*, **95**, 4802 (1991).

11) S. Ito, T. Tsunetsugu, T. Kanno, H. Sugiyama, and H. Takeshita, *Tetrahedron Lett.*, 3659 (1965).

12) R. L. Redington and C. W. Bock, *J. Phys. Chem.*, **95**, 10284 (1991).